14th MEETING OF THE SCIENTIFIC COMMITTEE

7 to 12 September 2026, Tórshavn, Faroe Islands

SC14 - SQ 04

Squid Assessment Using an Environment-dependent State-Space Biomass Dynamics Model

China

Assessment of Jumbo Squid in the Southeast Pacific Ocean Using a environment-dependent State-Space Biomass Dynamics Model

Gang Li[1,2], Mingfeng Jiang[2], Mengxiong Yuan[2], Xinjun Chen[1,2]

National Data Centre for Distant-Water Fisheries of China

Shanghai Ocean University

Executive Summary

To account for regional variation in fishing operations, this assessment combined CPUE series from the Peruvian and Chilean fleets with a gamma-distribution-standardized CPUE series from the Chinese squid-jigging fleet to construct relative abundance indices for *Dosidicus gigas*. Six environment-dependent scenarios were implemented within a Bayesian state-space surplus production model. All scenarios were evaluated using CPUE residual diagnostics and retrospective analysis, with no evidence of residual autocorrelation or a systematic retrospective pattern. The results indicated that, from 2012 through 2025, the Southeast Pacific stock was neither overfished nor subject to overfishing.

1. Introduction

The jumbo squid, *Dosidicus gigas*, is a highly migratory cephalopod distributed widely throughout the eastern Pacific Ocean, from California to southern Chile (Nigmatullin et al., 2001). It is a major fishery resource that supports coastal economies in Peru, Chile, and Ecuador and attracts substantial fishing effort from Asia-Pacific nations (Morales-Bojórquez & Pacheco-Bedoya, 2016). Its semelparous life history, rapid growth, and high environmental sensitivity contribute to pronounced interannual variability associated with ENSO-driven changes in sea surface temperature and chlorophyll-a concentration (Arkhipkin et al., 2021; Robinson et al., 2013). Genetic evidence further suggests that jumbo squid should be managed as a single fishery stock throughout the Southeast Pacific (Pardo-Gandarillas et al., 2025). Given the species' biological plasticity and fishery importance, this study integrated a Bayesian state-space surplus production model with continuous environmental covariates to assess the population dynamics of *D. gigas* in the Southeast Pacific Ocean.

2. Data

2.1 Catch and Effort Data

Total annual catches of jumbo squid in the Southeast Pacific Ocean during 2012–2025 were obtained from the SPRFMO Secretariat.

2.2 Abundance Index Data

The assessment used CPUE indices for the Chinese fleet, the Chilean artisanal jig fleet, the Chilean industrial trawl fleet, and the Peruvian fleet. Scenarios S1 and S3 used the first three indices, whereas S2 and S4 additionally incorporated the Peruvian index. Because the Peruvian CPUE series had not been standardized, its relative precision in the observation likelihood was set to 0.1 times that of the other indices. This down-weighting reduced its influence on the overall assessment while retaining the potential information it contained on changes in stock abundance.

The CPUE series for the Peruvian and Chilean fleets were provided by the SPRFMO Secretariat.

The Asian-fleet CPUE index was represented by data from the Chinese squid-jigging fleet. Records provided by the China Distant-Water Fisheries Association included fishing date, fishing location at a spatial resolution of 0.25° × 0.25°, and catch. Nominal CPUE was calculated as catch divided by fishing days. A generalized additive model (GAM) was used to standardize CPUE:

$$g(\mu_i) = \alpha + \sum f_i \times X_i + \varepsilon$$

where α is the intercept; f_i denotes the smooth function associated with covariate X_i; and ε_i is the error term, assumed to follow the specified statistical distribution. Candidate explanatory variables included environmental covariates (sea surface temperature (SST), chlorophyll-a concentration (Chl-a), sea surface salinity (SSS), and the Niño 1+2 index), spatiotemporal covariates (year, month, longitude, and latitude), and interaction terms. An El Niño event-level factor (ELE), derived from the Niño 1+2 index, was also evaluated as a candidate categorical climate covariate to determine whether discrete event classes provided information beyond the continuous index. CPUE was assumed to follow a gamma distribution. Zero nominal-CPUE observations were excluded before model fitting.

Environmental covariates were obtained from the NOAA Climate Prediction Center, the Copernicus Marine Service, and NASA databases (Table 1).

Table 1. Sources and Spatiotemporal Resolution of Marine Environmental Variables

Environmental variable	Source	Temporal/spatial resolution
Niño 1+2 index	https://www.cpc.ncep.noaa.gov/	Monthly
SST	https://data.marine.copernicus.eu/	Monthly; 0.083° × 0.083°
SSS	https://data.marine.copernicus.eu/	Monthly; 0.083° × 0.083°
Chl-a	https://data.marine.copernicus.eu/	Monthly; 0.25° × 0.25°
SSHA	https://podaac.jpl.nasa.gov/	Monthly; 0.25° × 0.25°

3. Model Development

3.1 Bayesian State-Space Surplus Production Model

An operational surplus production model consists of two components: a process model describing changes in stock biomass through production and removals, and an observation model linking observed abundance indices (e.g., fishery CPUE or survey indices) to stock biomass (Hilborn et al., 1992).

Pella and Tomlinson proposed the following extension of the Schaefer model:

$$B_{y+1} = (B_y + \frac{r}{s-1} B_y (1 - \left(\frac{B_y}{K}\right)^{s-1} - C_{y,i}\right) e^{\mu_y}$$

where B_Y is biomass at the beginning of year y; C_Y is the catch taken during year y; μ_Y is the process error, assumed to follow a normal distribution; r is the intrinsic population growth rate; and K is the carrying capacity, representing unexploited biomass.

The observation model was specified as:

$$I_{y,i} = q_i B_y \exp(\varepsilon_{y,i})$$

where i indexes fleets (Peru, China, Chilean artisanal jig, and Chilean industrial trawl); $I_{Y,i}$ is the abundance index for fleet i in year y; q_i is the fleet-specific catchability coefficient; and $\varepsilon_{Y,i}$ is the observation error, assumed to follow a normal distribution.

3.2 Environment-Dependent Surplus Production Model

Continuous environmental indices were used to drive the stock productivity parameter r and the catchability parameter q_i for each CPUE series. Before entering the model, each environmental series was divided by its sample standard deviation without mean centering. Consequently, an original environmental-index value of zero continued to represent neutral conditions.

$$E_{k,t}^{\star} = \frac{E_{k,t}}{\mathrm{SD}(E_k)}$$

where k identifies the environmental series used to drive r or a specific q_i.

The environmental model separately represented effects on stock productivity and catchability. Annual environment-dependent productivity was defined as:

$$r_t = r\exp\left(\beta_r E_{r,t}^{\star}\right)$$

The environment-dependent catchability for CPUE series i was defined as:

$$q_{i,t} = q_i\exp\left(\beta_{q_i} E_{q_i,t}^{\star}\right)$$

Parameters β_r and βq_i quantify the response of productivity and catchability, respectively, to the standardized environmental index. K and s were held constant across years. The transition from state t − 1 to t used r_{t-1}, representing the effect of environmental conditions in the preceding year on production in the current year.

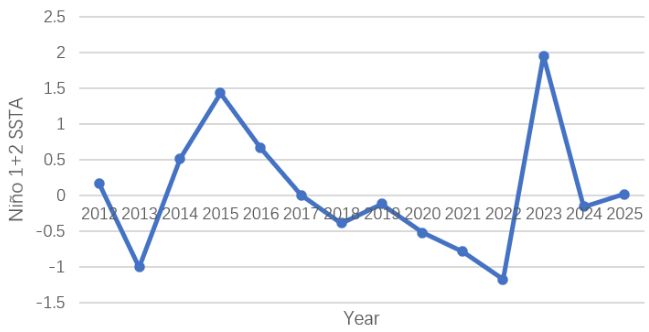

Figure 1. Annual Niño 1+2 SSTA from 2012 to 2025

3.3 Model Scenarios

The analysis first fitted four baseline Bayesian surplus production models without environmental covariates (S1–S4) to evaluate the effects of time-series length and inclusion of the Peruvian CPUE index. CPUE residual diagnostics were then conducted. Because several CPUE series in S3 and S4 exhibited temporal trends and cyclic patterns, these longer time-series models were not extended to include environmental effects. Environmental models were therefore developed only from S1 and S2, producing scenarios SE1–SE6. The retained models were subsequently evaluated through MCMC convergence diagnostics, prior–posterior comparisons, CPUE residual diagnostics, retrospective analysis, stock-status comparisons, TAC projections, and hockey-stick harvest-control-rule analyses.

Table 2. Baseline Model Scenarios Without Environmental Covariates

Model	Time period	CPUE combination	Weight of Peruvian CPUE	Subsequent use
S1	2012–2025	Chinese + Chilean artisanal + Chilean industrial	—	Developed into SE1–SE3
S2	2012–2025	S1 + Peruvian	0.1	Developed into SE4–SE6
S3	2003–2025	Chinese + Chilean artisanal + Chilean industrial	—	Baseline comparison and diagnostics only
S4	2003–2025	S3 + Peruvian	0.1	Baseline comparison and diagnostics only

Table 3. Environment-Dependent Model Scenarios

Model	Baseline model	Time period	No. of CPUE series	r	q_i
SE1	S1	2012–2025	3	Time-varying	Time-varying
SE2	S1	2012–2025	3	Time-varying	Constant
SE3	S1	2012–2025	3	Constant	Time-varying
SE4	S2	2012–2025	4	Time-varying	Time-varying
SE5	S2	2012–2025	4	Time-varying	Constant
SE6	S2	2012–2025	4	Constant	Time-varying

3.4 Prior Distributions

Model parameters were estimated within a Bayesian framework. Table 4 summarizes the principal prior distributions and parameter settings used in the current SE1 configuration. To maintain comparability among scenarios, the environmental variants used the same baseline priors wherever possible, with β_r and βq_i included or omitted according to model structure.

Table 4. Principal Prior Distributions and Parameter Settings

Parameter	Prior distribution/setting
r	Uniform(0.79, 1.79)

Parameter	Prior distribution/setting
β_r	Normal(0, 4)
K	Uniform(130, 1950)
s	Uniform(1, 5)
q_i	Uniform(0.001, 1)
βq_i	Normal(0, 4)
P initial	Uniform(0.001, 1)

3.5 Biological Reference Points and Stock Status

Under the Pella–Tomlinson parameterization, maximum sustainable yield reference points were calculated as:

$$B_{\text{MSY}} = Ks^{-1/(s-1)}$$

$$F_{\text{MSY},t} = \frac{r_t}{s}$$

$$\text{MSY}_t = B_{\text{MSY}} F_{\text{MSY},t}$$

When r was constant, F_MSY and MSY were constant across years. When r_t varied with environmental conditions, F_MSY,$_t$ and MSY$_t$ varied annually, whereas B_MSY remained determined by the time-invariant parameters K and s. Annual fishing mortality and relative stock-status indicators were defined as:

$$F_t = \frac{C_t}{B_t}$$

$$B_{\text{ratio},t} = \frac{B_t}{B_{\text{MSY}}} \quad ; \quad F_{\text{ratio},t} = \frac{F_t}{F_{\text{MSY},t}}$$

Terminal stock status was summarized from the posterior distributions of B_ratio and F_ratio and displayed using a Kobe plot.

3.6 Model Diagnostics and Selection

Model performance was evaluated at four levels:

- MCMC convergence: inspection of trace plots, Gelman–Rubin diagnostics (R-hat), and effective sample size.
- Prior–posterior information gain: comparison of prior and posterior densities and calculation of the posterior-to-prior variance ratio (PVR).
- CPUE residual diagnostics: examination of residual time series, linear trends, normal Q–Q plots, Shapiro–Wilk tests, residual autocorrelation functions, and Ljung–Box tests.
- Retrospective diagnostics: sequential removal of terminal-year data, comparison of B and F estimates for common historical years, and calculation of Mohn's ρ.

3.7 TAC Projections

Forward projections were conducted using posterior samples from each candidate model. Starting from the terminal stock state, candidate TACs were entered as annual removals in the state equation to generate posterior distributions of future B, F, Bratio, and Fratio. For models with time-varying r, the posterior distribution of terminal-year r_t was carried forward when independent forecasts of future environmental conditions were unavailable. When future environmental indices are available, r_t can be updated within the same model structure. Time-varying q affects only the observation process and therefore does not directly alter projected biomass dynamics.

The TAC analysis comprised a fixed TAC grid and cross-model comparisons. The risk curves used candidate TACs from 500 to 2,000 thousand t in increments of 100 thousand t and calculated the probabilities that future biomass would fall below B_{MSY} and that fishing mortality would exceed F_{MSY}. Results were reported separately for each environmental model and were also summarized using an equal-weight average across SE1–SE6.

Table 5. TAC Projection Scenarios

Item	Current setting	Output
Projection origin	Terminal assessment year: 2025	Posterior samples of B_2025 and model parameters
Projection horizon	2 years	Projected B, F, Bratio, and Fratio
Fixed TAC grid	50–200 × 10^4 t in increments of 10 × 10^4 t	Risk curves for each TAC
Risk metrics	Pr(B_ratio < 1), Pr(F_ratio > 1), and the probability of either event	Identification of risk thresholds and TAC intersections
Model averaging	Equal weights for SE1–SE6	Scenario-specific and combined results

3.8 Hockey-Stick Harvest Control Rule

The hockey-stick harvest control rule used B_{MSY} as the biomass trigger. When biomass was at or above B_{MSY}, target fishing mortality was set to F_{MSY}. When biomass fell below B_{MSY}, target fishing mortality declined linearly with relative biomass:

$$F_{\text{target},t} = F_{\text{MSY},t} \times \min\left(1, \frac{B_{t-1}}{B_{\text{trigger},t}}\right)$$

$$B_{\text{trigger},t} = B_{\text{MSY}}$$

Instantaneous fishing mortality was converted to an annual harvest fraction as:

$$u_{\text{target},t} = 1 - \exp\left(-F_{\text{target},t}\right)$$

$$\text{TAC}_t = B_{t-1} u_{\text{target},t}$$

The 2026 TAC was calculated from the estimated 2025 stock state, whereas the 2027 TAC was calculated from the stock state projected after implementation of the 2026 TAC.

4. Results

4.1 Generalized Additive Model

All covariate effects included in the GAM were statistically significant ($P < 0.01$). Candidate terms were added sequentially, and the final model, which included all significant terms, had the minimum AIC of 675,826 (Table 6). Nominal and standardized CPUE showed fluctuating temporal patterns. Their trends differed notably during 2012–2014 and 2021–2023, although both series reached their highest values in 2015 and their lowest values in 2024 (Figure 2).

Table 6. Results of GAM Model Selection

Term added	F or t statistic	P-value	Adjusted R^2	AIC	Cumulative deviance (%)	Incremental deviance (%)
Null model			0.0000	729,830.2	0.0000	0.0000
+Year	3.6000	<0.001	0.1340	702,616.8	14.6442	14.6442
+Month	-7.7100	<0.001	0.1913	688,995.4	21.2229	6.5787
+Spatial smooth	112.8	<0.001	0.2154	682,522.1	24.2176	2.9946
+SST	72.3200	<0.001	0.2197	681,231.3	24.8111	0.5935
+SSS	84.8900	<0.001	0.2253	679,880.3	25.4152	0.6041
+SSHA	60.2700	<0.001	0.2319	678,825.5	25.8932	0.4780
+Chl-a	24.1300	<0.001	0.2326	678,466.5	26.0631	0.1699
+Niño 1+2 SSTA	147.5	<0.001	0.2419	675,863.4	27.2083	1.1452
+ELE	4.5100	<0.001	0.2428	675,826.0	27.2262	0.0179

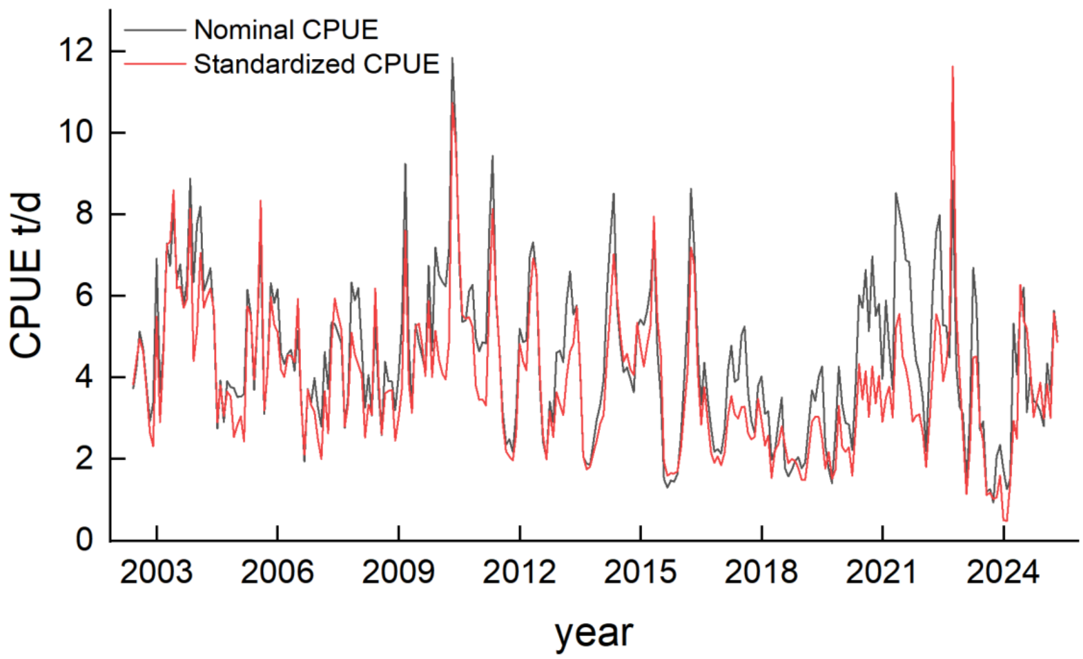

Figure 2. Nominal and Standardized CPUE Indices for Jumbo Squid

4.2 Parameter Estimates

The marked differences between the prior and posterior distributions indicated that the data substantially informed the posterior distributions of the estimated parameters (Figures 3–8).

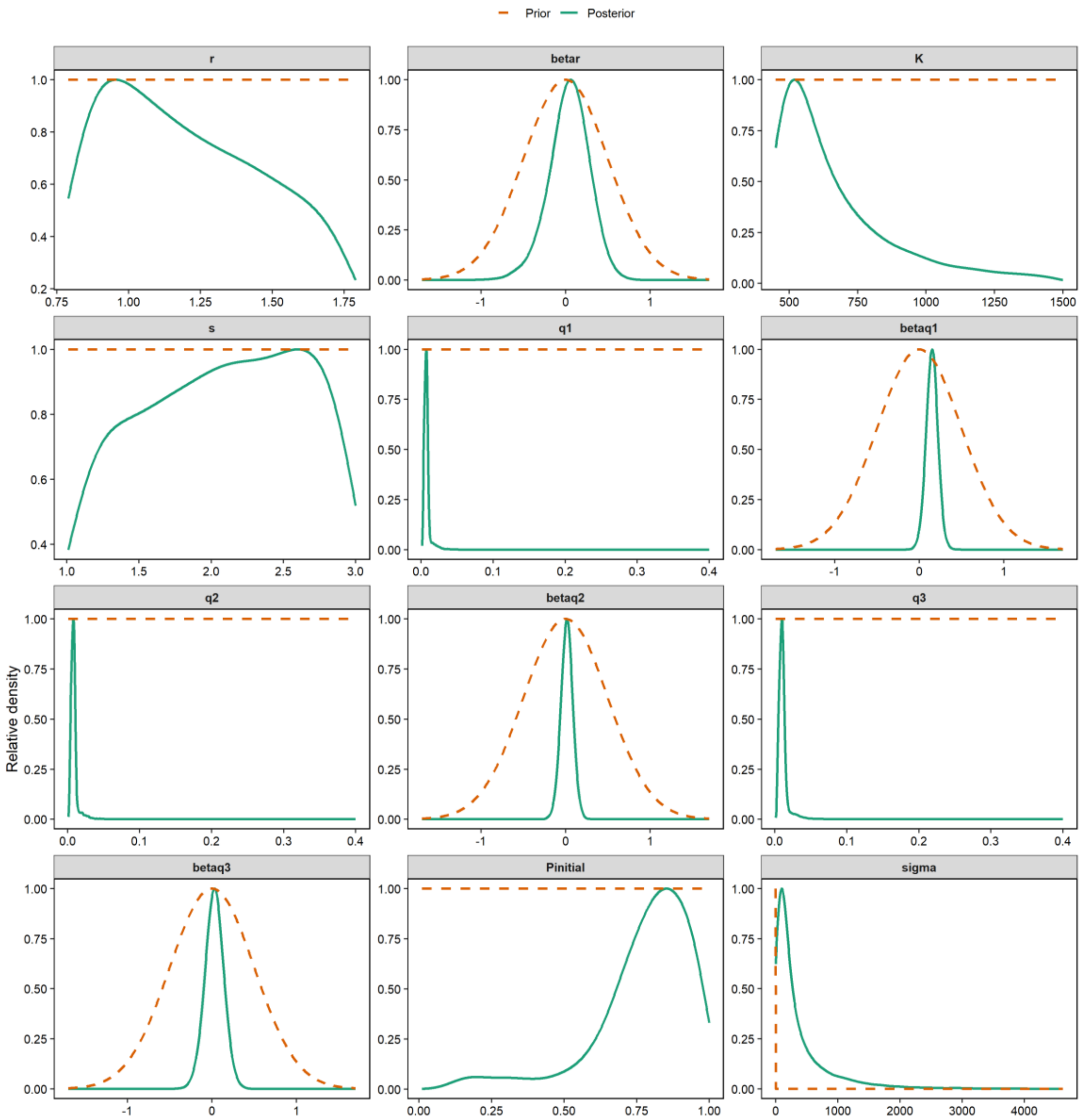

Figure 3. Prior and Posterior Distributions of Parameters for Scenario SE1

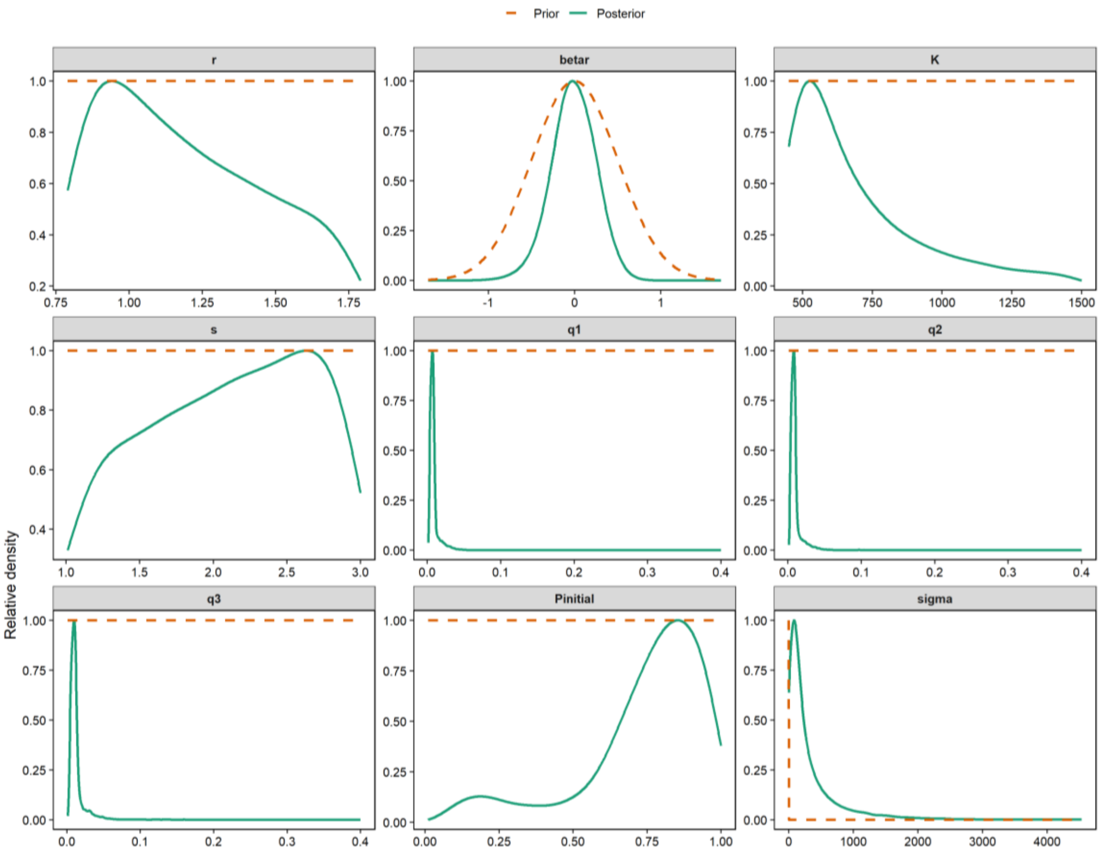

Figure 4. Prior and Posterior Distributions of Parameters for Scenario SE2

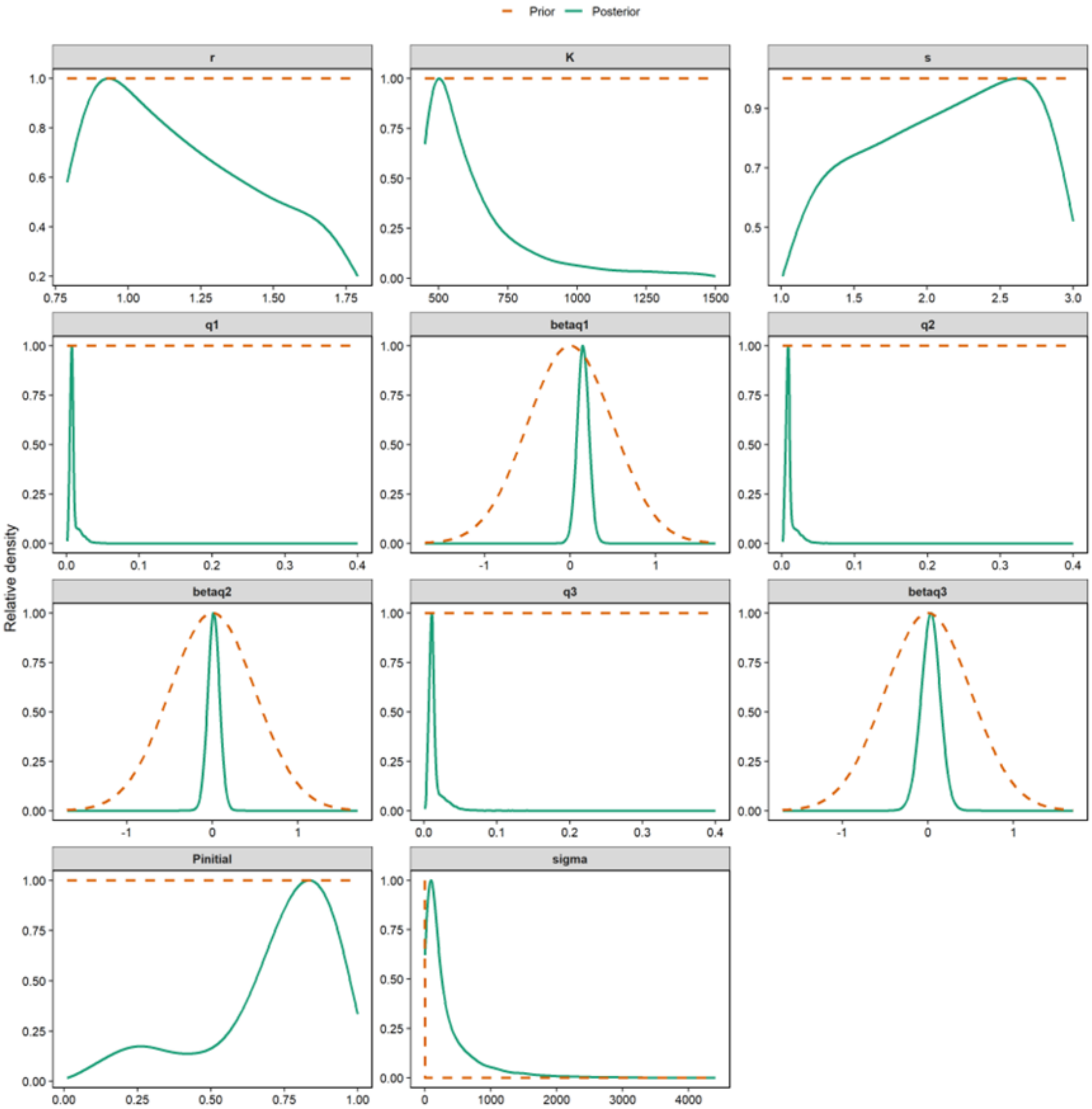

Figure 5. Prior and Posterior Distributions of Parameters for Scenario SE3

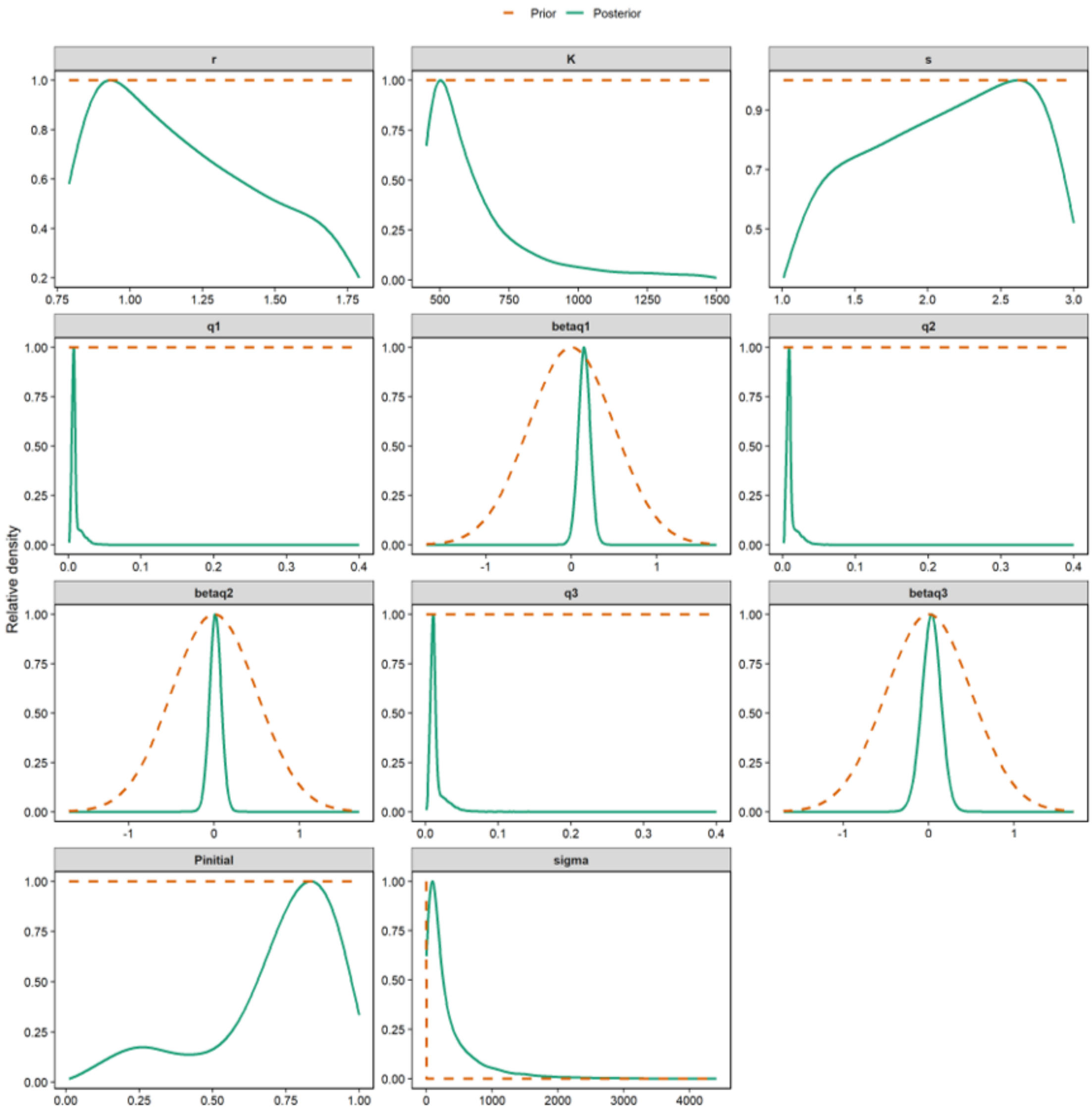

Figure 6. Prior and Posterior Distributions of Parameters for Scenario SE4

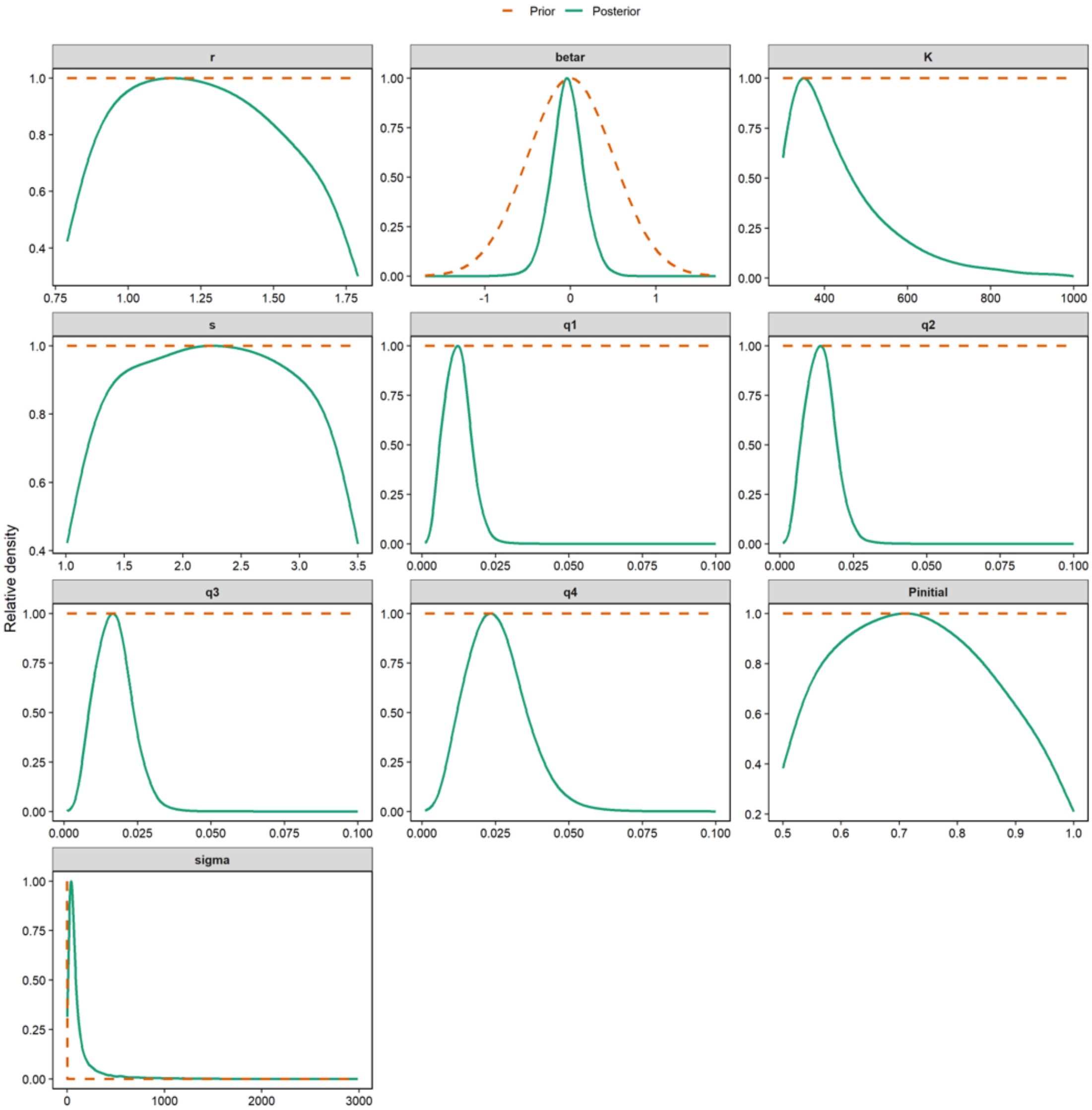

Figure 7. Prior and Posterior Distributions of Parameters for Scenario SE5

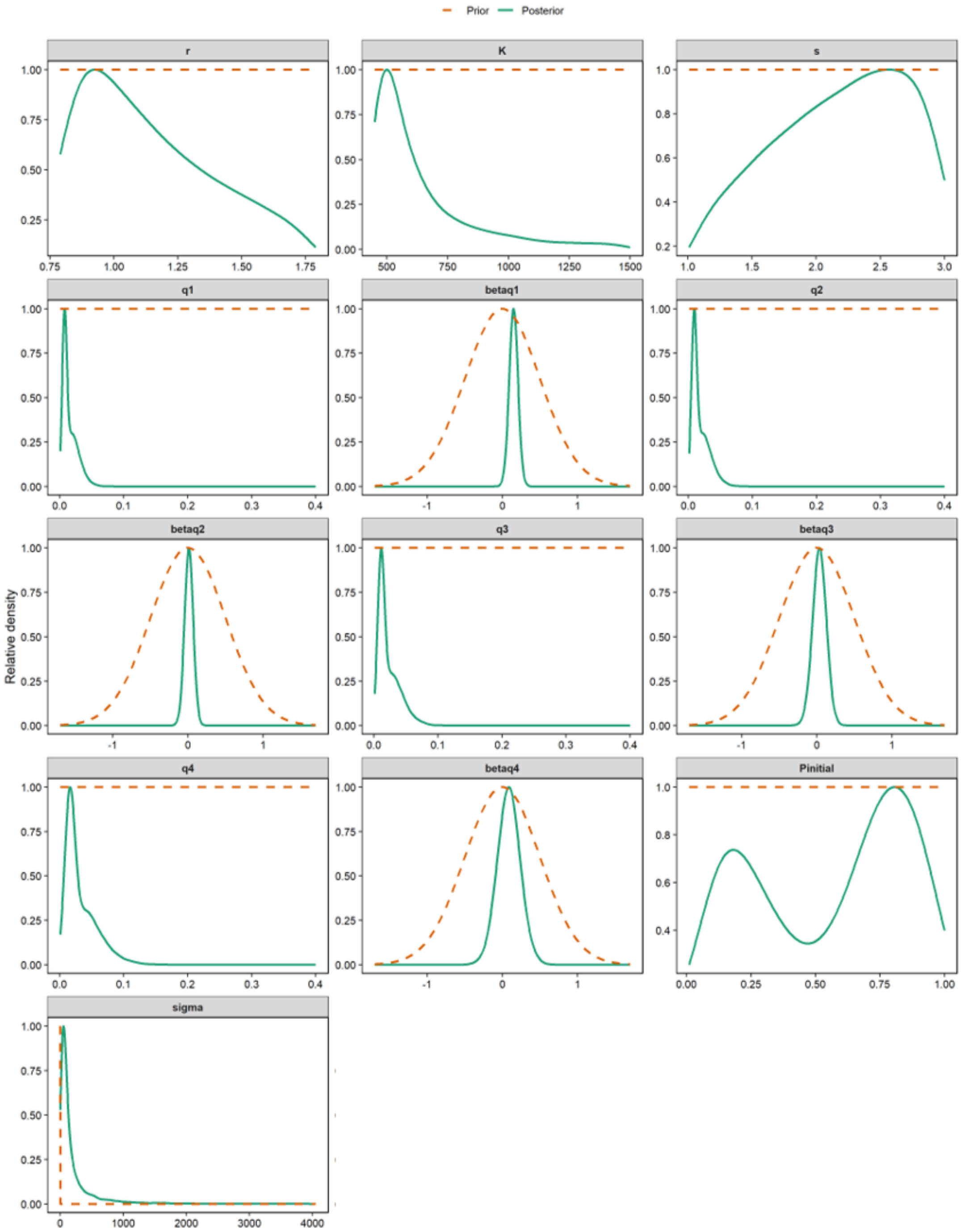

Figure 8. Prior and Posterior Distributions of Parameters for Scenario SE6

Table 7. Posterior Parameter Estimates for Scenario SE1

Statistic	r	β_r	K	s	q_1	βq_1	q_2	βq_2	q_3	βq_3	MSY (2025)	F_ratio (2025)	B_ratio (2025)
mean	1.24	0.05	737.26	3.05	0.006105	0.148265	0.007012	0.012228	0.00885	0.027012	182.2656	0.58	1.68
2.5%	0.81	-0.51	425.89	1.12	0.002858	0.009612	0.003274	-0.1245	0.004053	-0.1889	88.46975	0.14	0.80
25%	1.06	-0.11	587.1	2.09	0.00437	0.1026	0.005032	-0.03274	0.006309	-0.04554	122.9	0.31	1.37
50%	1.22	0.07	706.35	3.08	0.005582	0.1489	0.006413	0.01186	0.008069	0.026965	160.6	0.49	1.63
75%	1.4	0.23	850.8	4.03	0.007221	0.1941	0.008296	0.056545	0.01049	0.1002	218.5	0.75	1.96
97.5%	1.83	0.53	1239	4.89	0.01254	0.2834	0.01439	0.1483	0.0183	0.242305	398.7025	1.54	2.76

4.3 Model Diagnostics

CPUE residual diagnostics indicated a slight but statistically significant trend for the Chilean artisanal-fleet CPUE in all six scenarios, consistent with systematic overestimation. No significant temporal trend was detected for the other CPUE series, and no residual autocorrelation was observed in any scenario (Figures 9–14). A three-peel retrospective analysis of SE1 showed no evidence of a systematic retrospective pattern (Figure 15).

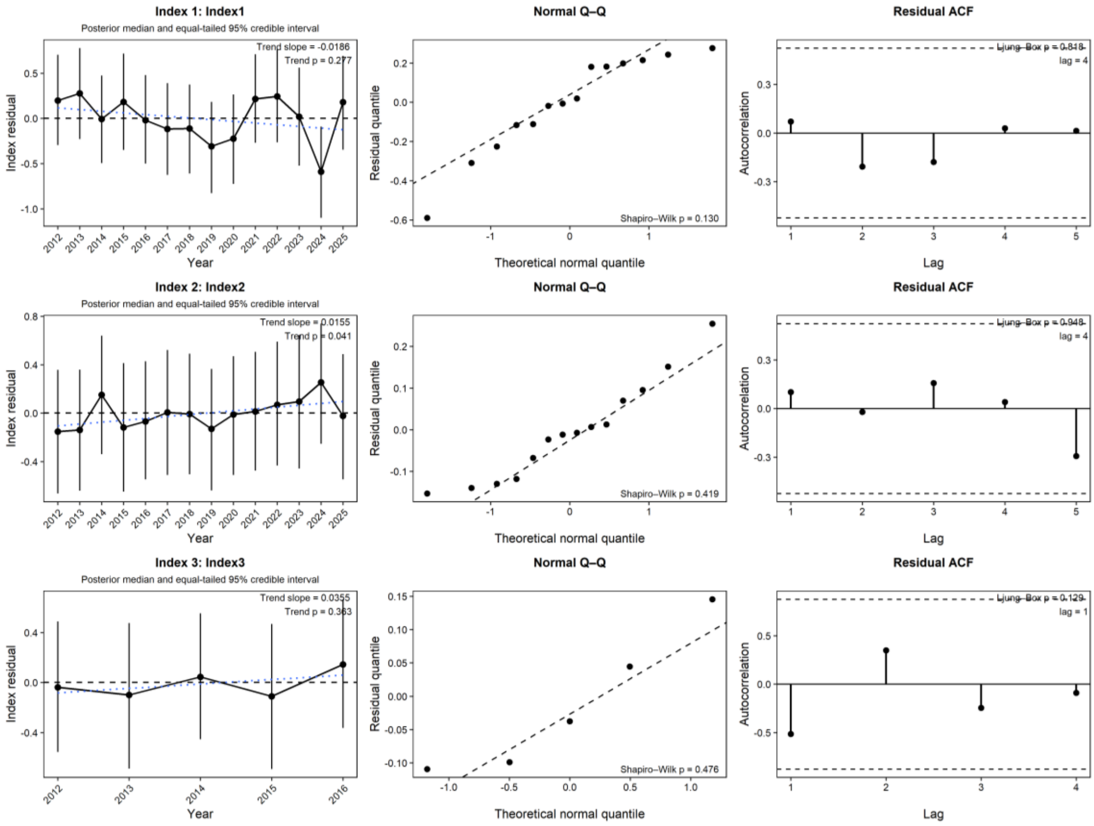

Figure 9. CPUE Residual Diagnostics for Scenario SE1

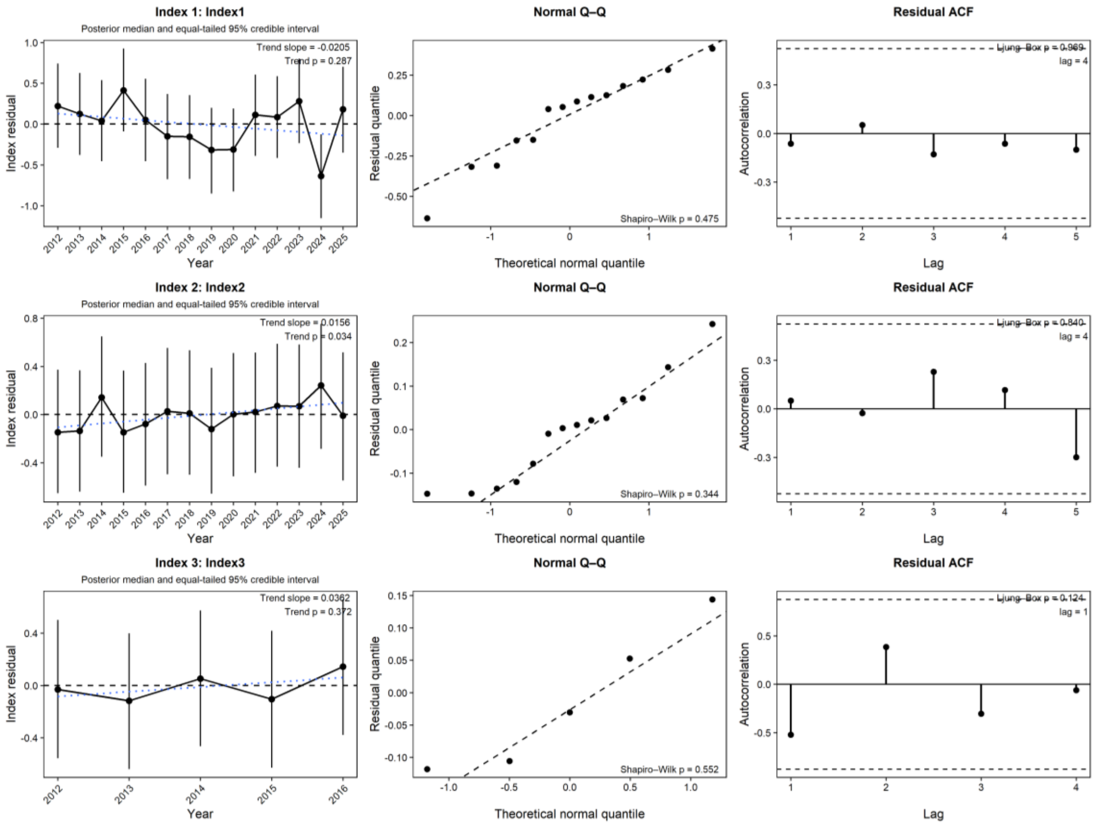

Figure 10. CPUE Residual Diagnostics for Scenario SE2

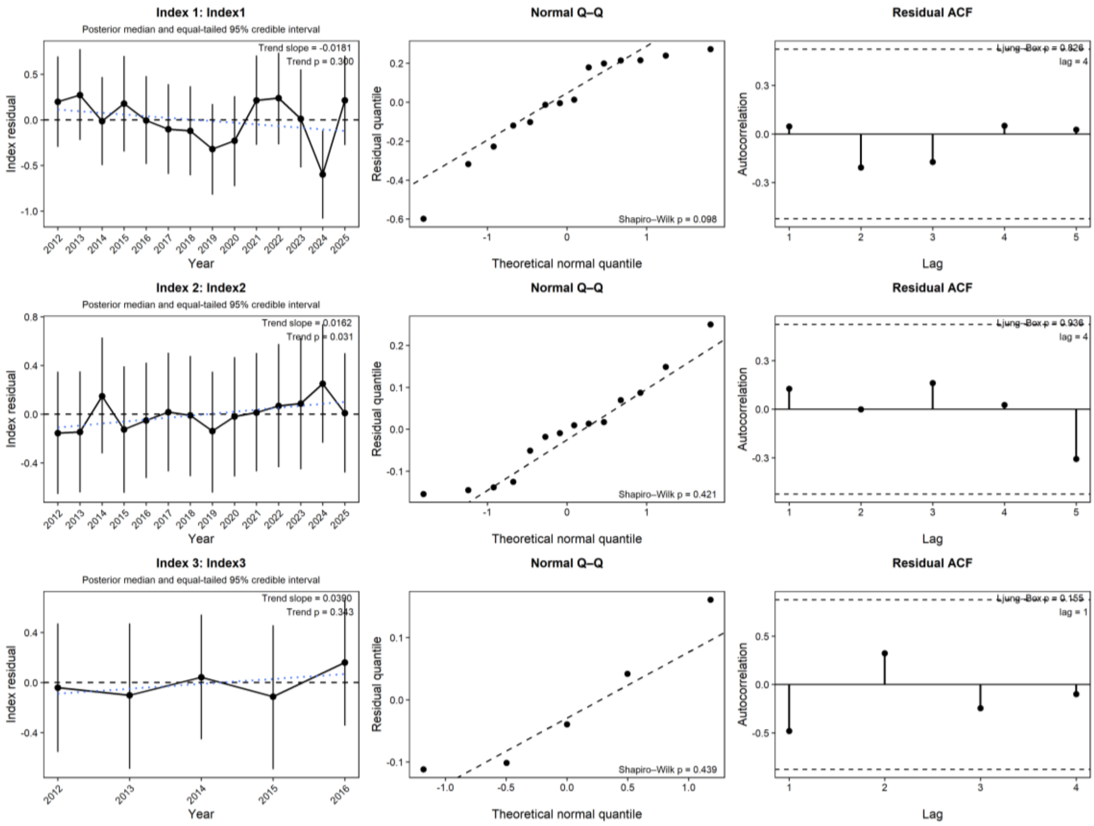

Figure 11. CPUE Residual Diagnostics for Scenario SE3

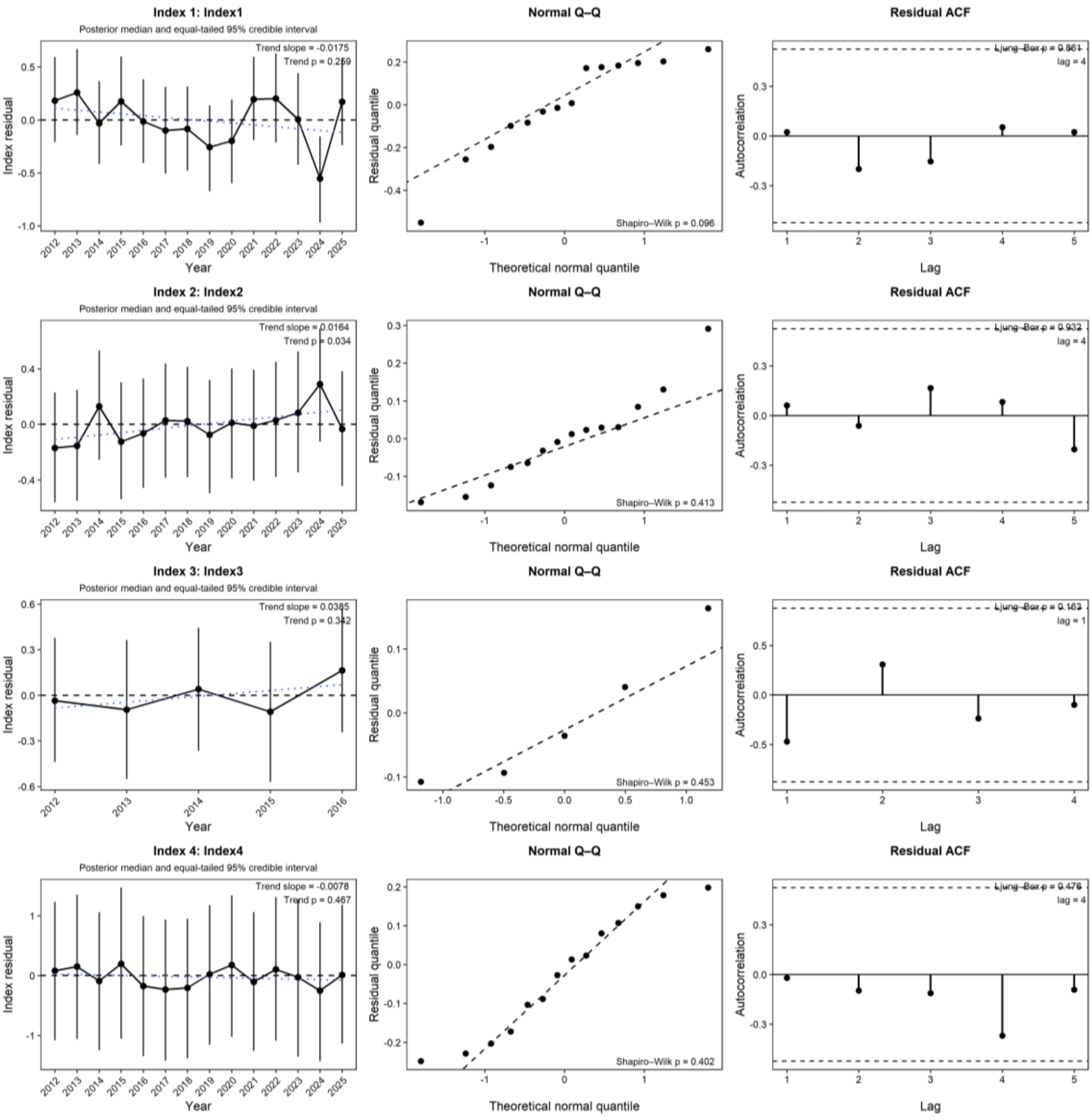

Figure 12. CPUE Residual Diagnostics for Scenario SE4

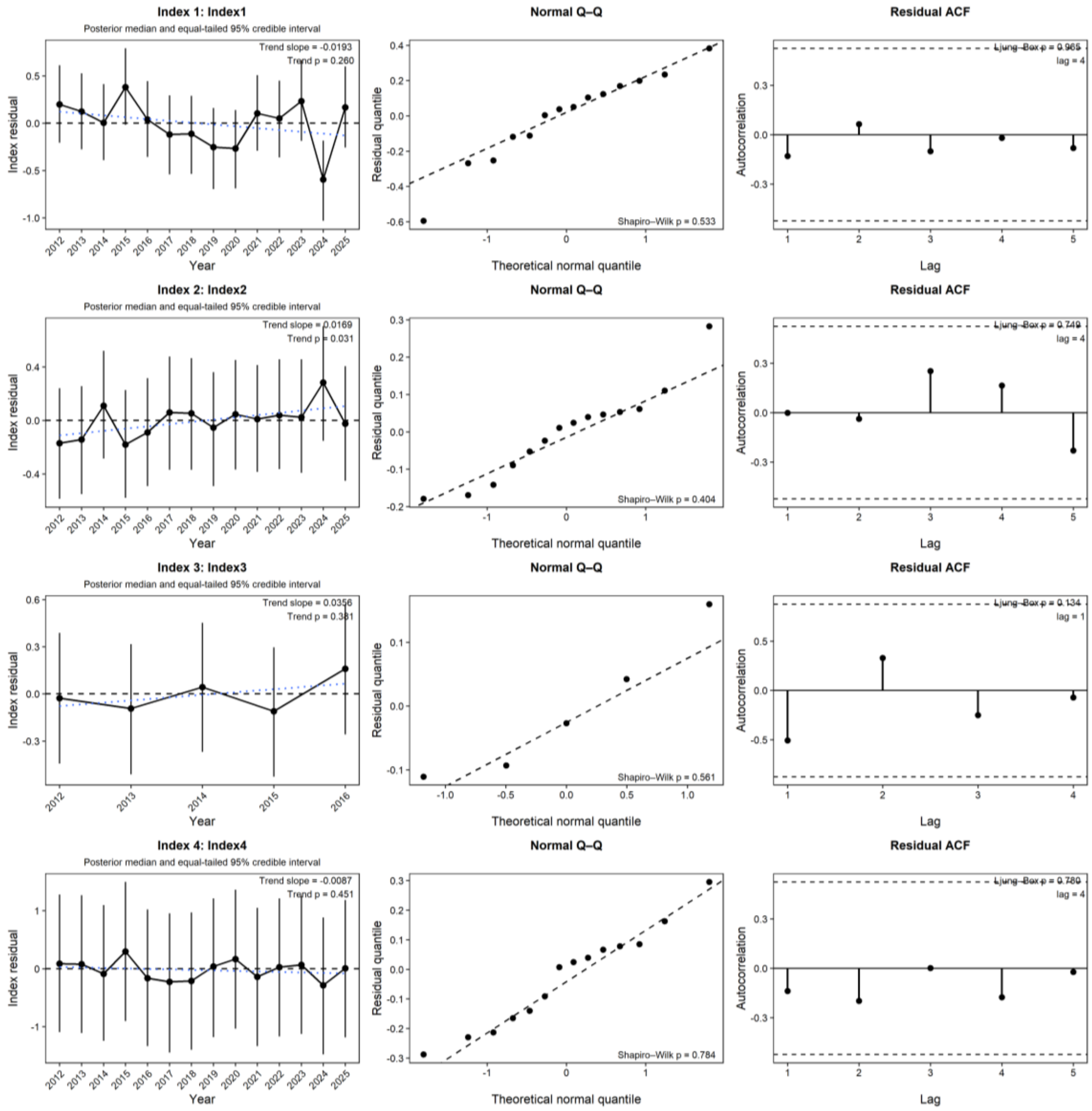

Figure 13. CPUE Residual Diagnostics for Scenario SE5

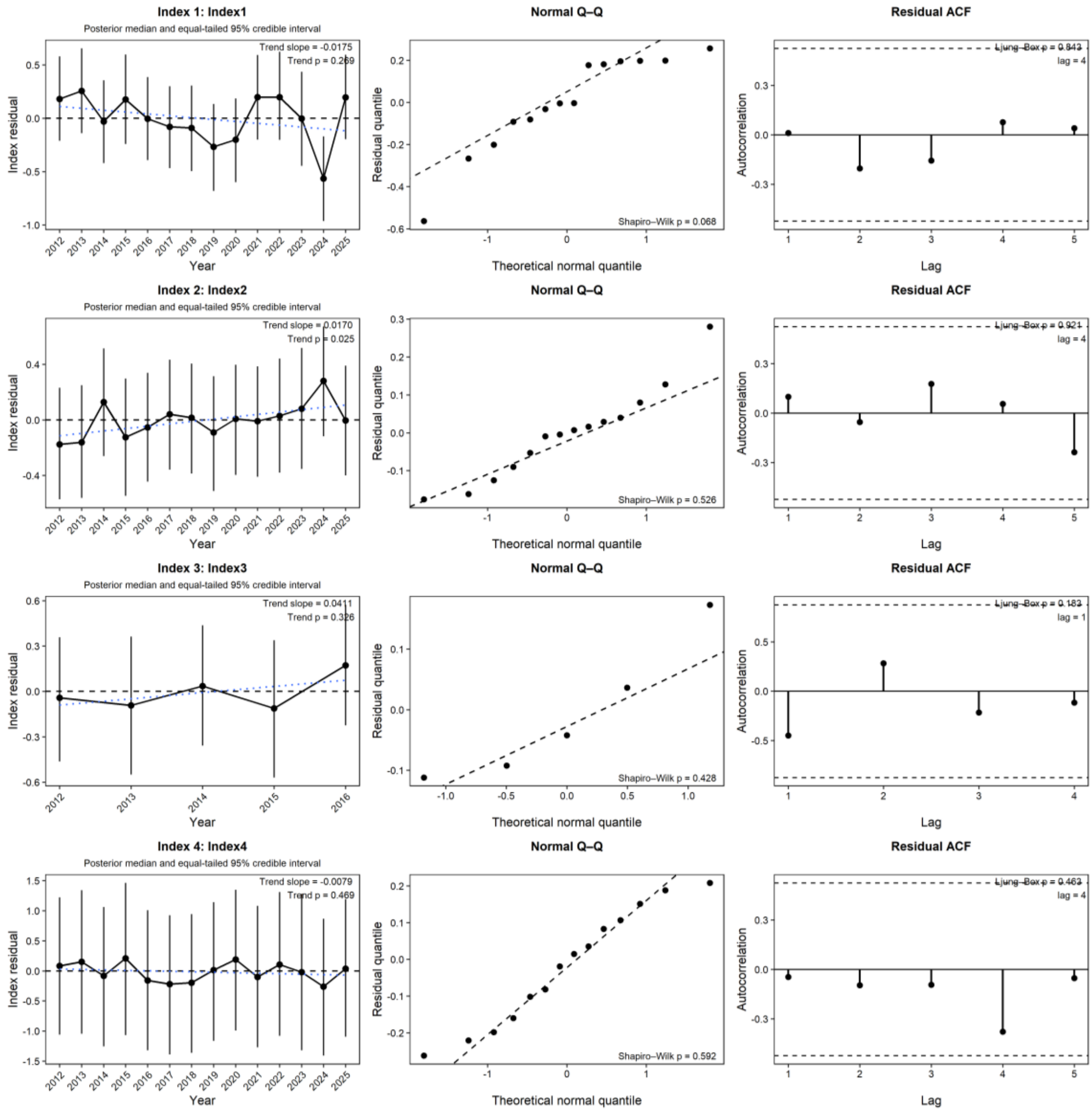

Figure 14. CPUE Residual Diagnostics for Scenario SE6

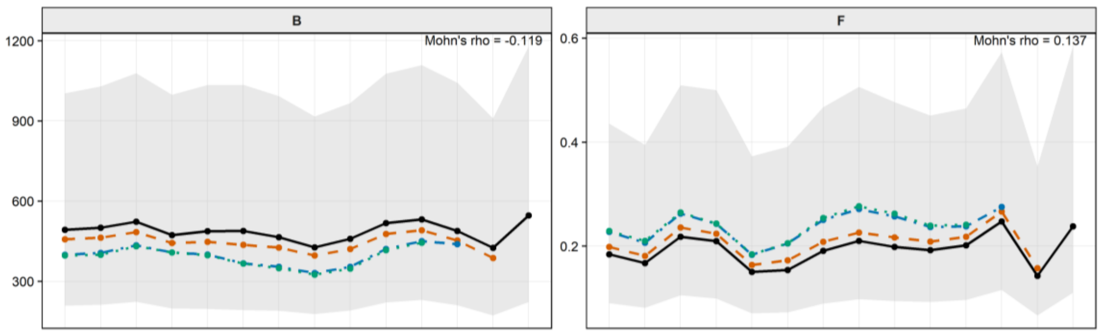

Figure 15. Three-Peel Retrospective Analysis for Scenario SE1

4.4 Stock Status

Time series of Bratio and Fratio showed consistent patterns across all scenarios (Figure 16). The combined Kobe plot indicated that the stock remained in the sustainable quadrant in 2025, with neither an overfished condition nor overfishing (Figure 17).

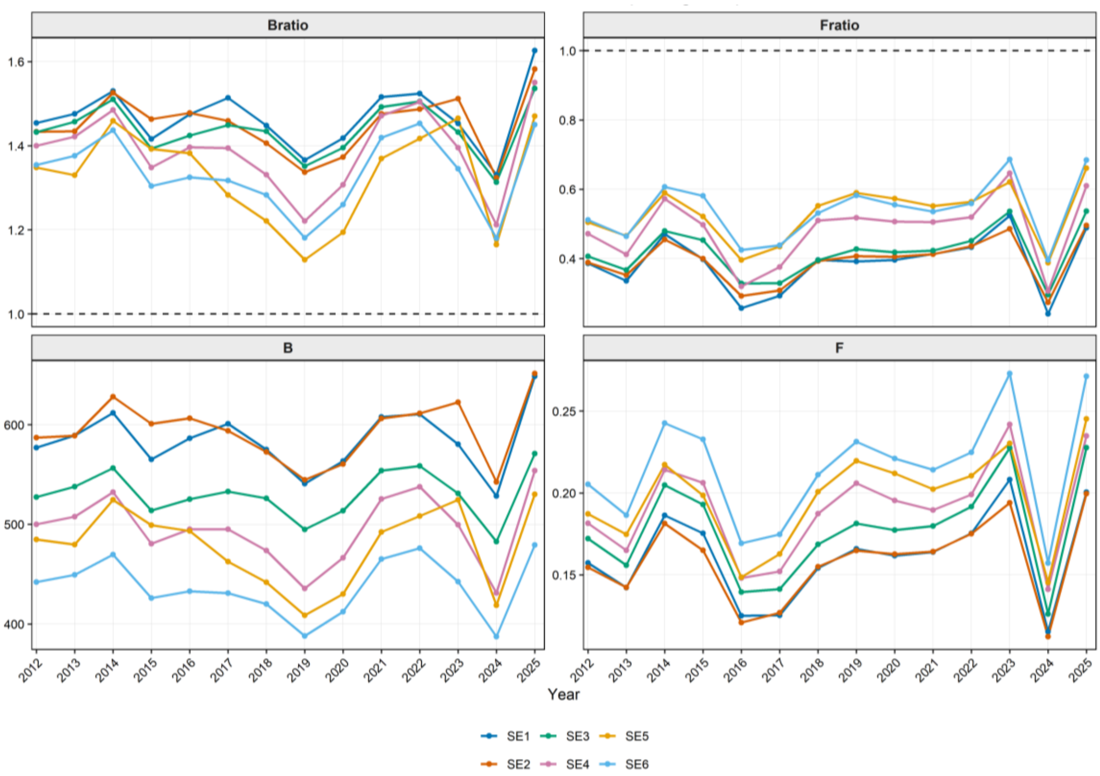

Figure 16. Time Series of B_ratio, F_ratio, Biomass (B), and Fishing Mortality (F) Across All Scenarios, 2012–2025

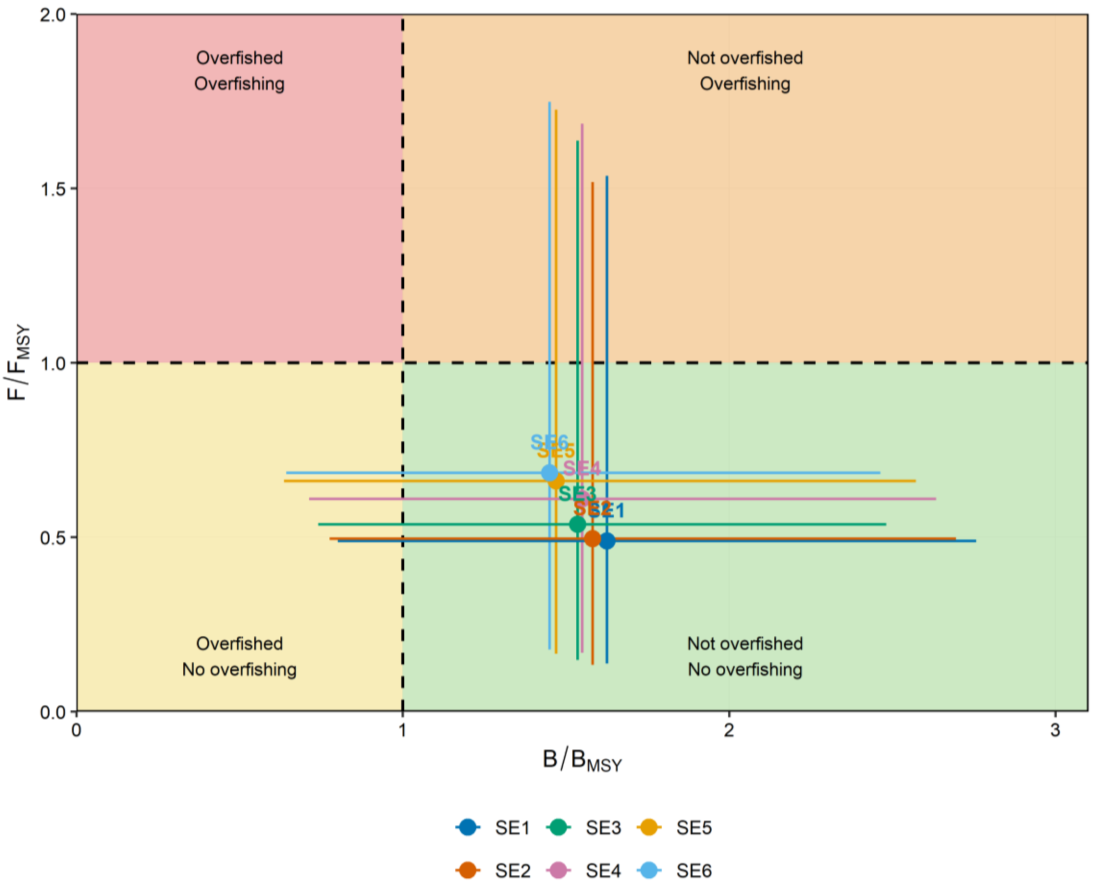

Figure 17. Combined Kobe Plot for All Scenarios

4.5 TAC Risk Analysis

The grid-based TAC risk analysis identified advisory TACs of 1,771 thousand t for 2026 and 1,644 thousand t for 2027 as the levels associated with the selected threshold for avoiding both an overfished condition and overfishing (Figure 18).

Under the hockey-stick harvest control rule, advisory TACs of 1,881 thousand t for 2026 and 1,333 thousand t for 2027 were estimated to maintain stock sustainability (Figure 19).

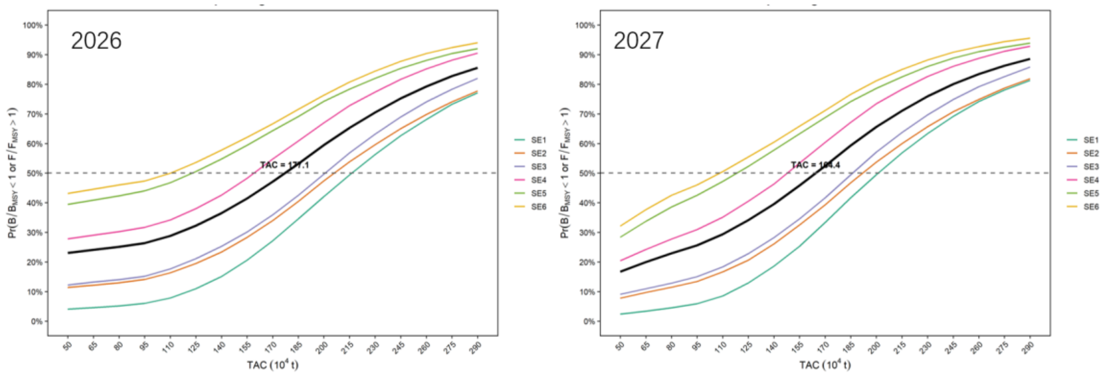

Figure 18. TAC Risk Curves for 2026 and 2027 Under Scenarios SE1–SE6 and Their Equal-Weight Average

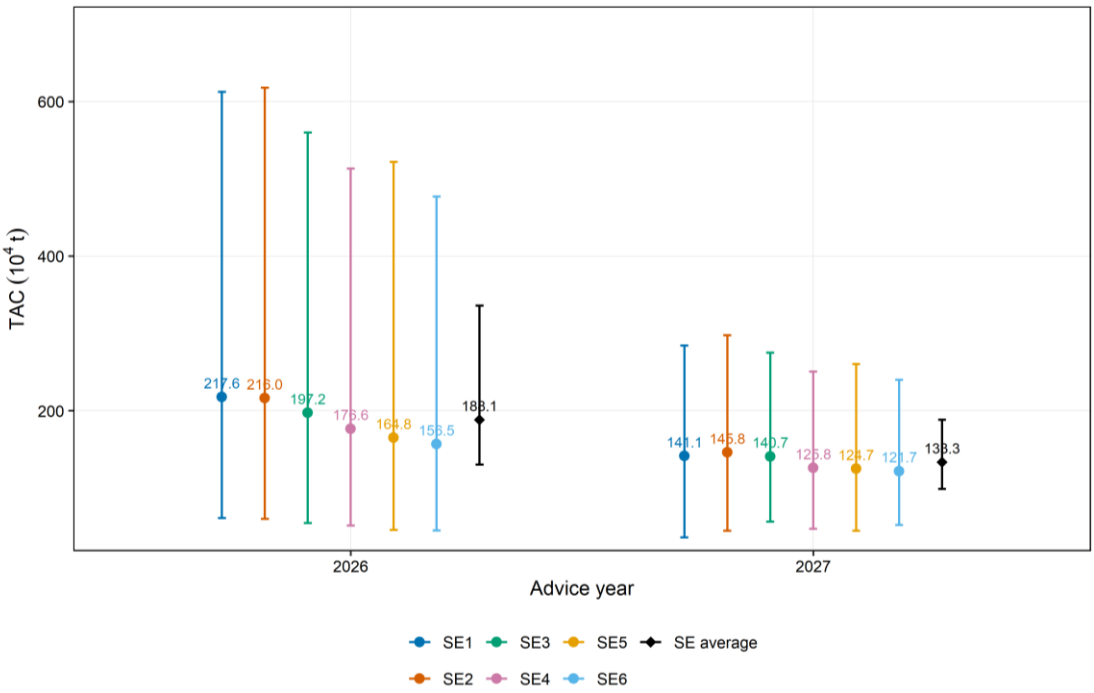

Figure 19. Hockey-Stick TAC Advice for 2026 and 2027 Under Scenarios SE1–SE6 and Their Equal-Weight Average

References

Arkhipkin, A. I., Hendrickson, L. C., Payá, I., Pierce, G. J., Roa-Ureta, R. H., Robin, J. P., & Winter, A. (2021). Stock assessment and management of cephalopods: advances and challenges for short-lived fishery resources. *ICES Journal of Marine Science*, *78*(2), 714-730.

Morales-Bojórquez, E., & Pacheco-Bedoya, J. L. (2016). Jumbo squid Dosidicus gigas: a new fishery in Ecuador. *Reviews in Fisheries Science & Aquaculture*, *24*(1), 98-110.

Nigmatullin, C. M., Nesis, K. N., & Arkhipkin, A. I. (2001). A review of the biology of the jumbo squid Dosidicus gigas (Cephalopoda: Ommastrephidae). *Fisheries Research*, *54*(1), 9-19.

Pardo-Gandarillas, M. C., Márquez-Gajardo, C., Morales, P., Catalán, J., Poni, K., Rosenfeld, S., ... & Ibáñez, C. M. (2025). Tracing Ice-Age legacies: phylogeography and glacial refugia of the endemic chiton Tonicina zschaui (Polyplacophora: Ischnochitonidae) in the West Antarctic Region. *Diversity*, *17*(9), 626.